Development and Testing of the OPLS All-Atom Force Field on Conformational Energetics and Properties of Organic Liquids

William L. Jorgensen,* David S. Maxwell, and Julian Tirado-Rives

Contribution from the Department of Chemistry, Yale University, New Haven, Connecticut 06520-8107

Received June 27, 1996. Revised Manuscript Received September 5, 1996[⊗]

Abstract: The parametrization and testing of the OPLS all-atom force field for organic molecules and peptides are described. Parameters for both torsional and nonbonded energetics have been derived, while the bond stretching and angle bending parameters have been adopted mostly from the AMBER all-atom force field. The torsional parameters were determined by fitting to rotational energy profiles obtained from ab initio molecular orbital calculations at the RHF/6-31G*//RHF/6-31G* level for more than 50 organic molecules and ions. The quality of the fits was high with average errors for conformational energies of less than 0.2 kcal/mol. The force-field results for molecular structures are also demonstrated to closely match the ab initio predictions. The nonbonded parameters were developed in conjunction with Monte Carlo statistical mechanics simulations by computing thermodynamic and structural properties for 34 pure organic liquids including alkanes, alkenes, alcohols, ethers, acetals, thiols, sulfides, disulfides, aldehydes, ketones, and amides. Average errors in comparison with experimental data are 2% for heats of vaporization and densities. The Monte Carlo simulations included sampling all internal and intermolecular degrees of freedom. It is found that such non-polar and monofunctional systems do not show significant condensed-phase effects on internal energies in going from the gas phase to the pure liquids.

Introduction

Computer modeling of fluid systems is now commonplace with applications ranging from elucidating the structures and properties of pure liquids to predictions on protein stability and ligand binding.[1] The principal computational methods are molecular dynamics (MD) and Monte Carlo statistical mechanics (MC) in a classical framework.[2] The outcome of the simulations is primarily controlled by the expressions for the total energy, which are collectively referred to as the force field. Most force fields in widespread use for macromolecular systems have a similar form including harmonic bond stretching and angle bending, Fourier series for torsional energetics, and Coulomb plus Lennard-Jones terms for intermolecular and intramolecular nonbonded interactions.[3−6] Anharmonic and cross-terms may be added.[7] The incorporation of instantaneous polarization effects is also desirable and is being pursued, though it is not yet widely adopted owing to increased computational demands and a lack of fully developed polarizable force fields.[8,9] The differences for the non-polarizable force fields are mainly in choices on the numbers of interaction sites and the origin and extent of testing of the parameters in the energy expressions. Our efforts, as embodied in the development of the TIP3P and TIP4P models for water[10] and the OPLS force field for organic and biomolecular systems, have emphasized the importance of conformational energetics, basic intermolecular energetics in the gas phase, and the value of testing the force field on thermodynamic properties of pure organic liquids, especially heats of vaporization and densities,[11−15] and on free energies of hydration.[16] Correct representation of the latter properties gives confidence in the description of nonbonded interactions including hydrogen bonding and in the size of molecules. It should be obvious that force fields intended for use in simulations of fluid systems should be tested by making predictions on

[⊗] Abstract published in *Advance ACS Abstracts,* October 15, 1996.

(1) (a) Brooks, C. L., III; Pettitt, B. M.; Karplus, M. *Adv. Chem. Phys.* **1988**, *71*, 1. (b) Jorgensen, W. L. *Acc. Chem. Res.* **1989**, *22*, 184. (c) Kollman, P. A. *Chem. Rev.* **1993**, *93*, 2395. (d) Brünger, A. T.; Nilges, M. *Q. Rev. Biophys.* **1993**, *26*, 49.

(2) Allen, M. P.; Tildesley, D. J. *Computer Simulations of Liquids*; Clarendon Press: Oxford, UK, 1987.

(3) (a) Weiner, S. J.; Kollman, P. A.; Case, D. A.; Singh, U. C.; Ghio, C.; Alagona, G.; Profeta, S.; Weiner, P. J. *J. Am. Chem. Soc.* **1984**, *106*, 765. (b) Weiner, S. J.; Kollman, P. A.; Nguyen, D. T.; Case, D. A. *J. Comput. Chem.* **1986**, *7*, 230. (c) Cornell, W. D.; Cieplak, P.; Bayly, C. I.; Gould, I. R.; Merz, K. M., Jr.; Ferguson, D. M.; Spellmeyer, D. C.; Fox, T.; Caldwell, J. W.; Kollman, P. A. *J. Am. Chem. Soc.* **1995**, *117*, 5179.

(4) (a) Brooks, B. R.; Bruccoleri, R. E.; Olafson, B. D.; States, D. J.; Swaminathan, S.; Karplus, M. *J. Comp. Chem.* **1983**, *4*, 187. (b) Dunbrack, R.; Karplus, M. *Nature Struct. Biol.* **1994**, *1*, 334. MacKerell, A. D., Jr. Private communication.

(5) Mayo, S. L.; Olafson, B. D.; Goddard, W. A., III *J. Phys. Chem.* **1990**, *94*, 8897.

(6) Hagler, A. T.; Huler, E.; Lifson, S. *J. Am. Chem. Soc.* **1974**, *96*, 5319. Lifson, S.; Hagler, A. T.; Dauber, P. *J. Am. Chem. Soc.* **1979**, *101*, 5111.

(7) See: Halgren, T. A. *J. Comput. Chem.* **1996**, *17*, 490 and references therein.

(8) (a) van Belle, D.; Wodak, S. J. *J. Am. Chem. Soc.* **1993,** *115*, 647. (b) Caldwell, J. W.; Kollman, P. A. *J. Am. Chem. Soc.* **1995**, *117*, 4177.

(9) Jorgensen, W. L.; McDonald, N. A.; Selmi, M.; Rablen, P. R. *J. Am. Chem. Soc.* **1995**, *117*, 11809.

(10) Jorgensen, W. L.; Chandrasekhar, J.; Madura, J. D.; Impey, R. W.; Klein, M. L. *J. Chem. Phys.* **1983**, *79*, 926. Jorgensen, W. L.; Madura, J. D. *Mol. Phys.* **1985**, *56*, 1381.

(11) Jorgensen, W. L.; Madura, J. D.; Swenson, C. J. *J. Am. Chem. Soc.* **1984**, *106*, 6638.

(12) (a) Jorgensen, W. L. *J. Phys. Chem.* **1986**, *90*, 1276. (b) Jorgensen, W. L. *J. Phys. Chem.* **1986**, *90*, 6379. (c) Briggs, J. M.; Matsui, T.; Jorgensen, W. L. *J. Comput. Chem.* **1990**, *11*, 958. (d) Briggs, J. M.; Nguyen, T. B.; Jorgensen, W. L. *J. Phys. Chem.* **1991**, *95*, 3315.

(13) Jorgensen, W. L.; Swenson, C. J. *J. Am. Chem. Soc.* **1985**, *107*, 569, 1489.

(14) Jorgensen, W. L.; Severance, D. L. *J. Am. Chem. Soc.* **1990**, *112*, 4768. Jorgensen, W. L.; Nguyen, T. B. *J. Comput. Chem.* **1993**, *14*, 195. Pranata, J.; Wierschke, S. G.; Jorgensen, W. L. *J. Am. Chem. Soc.* **1991**, *113*, 2810.

(15) Jorgensen, W. L.; Tirado-Rives, J. *J. Am. Chem. Soc.* **1988**, *110*, 1657.

(16) Jorgensen, W. L.; Tirado-Rives, J. *Perspec. Drug. Discovery Des.* **1995**, *3*, 123.

S0002-7863(96)02176-2 CCC: $12.00

experimentally well-determined properties of fluids. Comparisons of computed and experimental results for solids can also be productive,[6,15] though experimental energetic data on solids is limited and the convergence of simulations of solids can be challenging.

The original OPLS (optimized potentials for liquid simulations) potential functions used a partially united-atom (UA) model; sites for nonbonded interactions are placed on all nonhydrogen atoms and on hydrogens attached to heteroatoms or carbons in aromatic rings.[11−15] Thus, the only hydrogens that are implicit are attached to aliphatic carbons. The computation time for fluid simulations is roughly proportional to the total number of interaction sites squared. Thus, the OPLS-UA model is computationally attractive, since, for example, the number of interaction sites for a molecule such as a propanol is 5 instead of 12 in an all-atom (AA) representation. The focus in development of the OPLS-UA model was on the nonbonded parameters, which historically had been the most problematic, and the new approach was to perform large numbers of Monte Carlo simulations of pure organic liquids for their refinement. For organic systems, the only internal degrees of freedom that were varied were torsions. The torsional energy terms were developed in an ad hoc manner by fitting to experimental or computational results for conformational energy profiles, which were considered to be the most reliable at the time.[11−14] The results were gratifying with average errors of ca. 2% for densities and heats of vaporization[10−14] and 1.0 kcal/mol for free energies of hydration.[16] For peptides and proteins, the OPLS nonbonded parameters were merged with the description of bond stretching, angle bending, and torsional energetics from the AMBER united-atom force field[3a] to yield the OPLS/AMBER force field.[15] It has seen widespread use after the original testing on conformational energetics for dipeptides and on the structures and unit-cell dimensions for crystals of cyclic peptides.[15]

Nevertheless, the added sites in all-atom models allow more flexibility for charge distributions and torsional energetics. This has been pursued and results have been reported for hydrocarbons with an OPLS-AA model; improved accord was obtained with experiment in several areas, particularly for the free energies of hydration of alkanes for which the average error was reduced from 0.9 to 0.3 kcal/mol.[17] As described here, this work has been extended to cover many common organic functional groups and all organic components needed for a protein force field. Besides parametrization of the nonbonded interactions, torsional potential functions have been obtained in a uniform manner by fitting to conformational energy profiles from ab initio RHF/6-31G*//RHF/6-31G* calculations for over 50 organic molecules and ions.[18] The torsional energetics at this level are in good agreement with experimental data and show little improvement with inclusion of MP2 correlation corrections.[18] The simultaneous parametrization of the nonbonded and torsional energy terms is desirable since they are coupled in the description of intramolecular energetics. The bond stretching and angle bending terms are more standardized and have largely been adopted from the AMBER AA force field.[3b] Continuing with the OPLS philosophy, the parametrization of the AA force field has included MC simulations for 34 organic liquids: ethane, propane, butane, isobutane, cyclohexane, propene, *trans*-2-butene, methanol, ethanol, propanol, 2-propanol, 2-methyl-2-propanol (*t*-BuOH), phenol, methanethiol, ethanethiol, propanethiol, dimethyl sulfide, ethyl methyl sulfide, dimethyl disulfide, acetamide, *N*-methylacetamide (NMA), *N*-methylpropanamide (NMP), *N*,*N*-dimethylacetamide (DMA), dimethyl ether (DME), ethyl methyl ether (EME), diethyl ether (DEE), tetrahydrofuran (THF), dimethoxymethane (DMM), 1,3-dioxolane, acetic acid, acetaldehyde, propanal, acetone, and butanone. Presentation of the force field and the results on conformational energetics and liquid properties are the focus of this paper.

Computational Methods

Force Field. The nonbonded interactions are represented by the Coulomb plus Lennard-Jones terms in eq 1, where E_{ab} is the interaction energy between molecules a and b.

$$E_{ab} = \sum_{i}^{\text{on a}} \sum_{j}^{\text{on b}} [q_i q_j e^2 / r_{ij} + 4\epsilon_{ij}(\sigma_{ij}^{12}/r_{ij}^{12} - \sigma_{ij}^{6}/r_{ij}^{6})] f_{ij} \qquad (1)$$

Standard combining rules are used such that $\sigma_{ij} = (\sigma_{ii}\sigma_{jj})^{1/2}$ and $\epsilon_{ij} = (\epsilon_{ii}\epsilon_{jj})^{1/2}$. The same expression is used for intramolecular nonbonded interactions between all pairs of atoms ($i < j$) separated by three or more bonds. Furthermore, $f_{ij} = 1.0$ except for intramolecular 1,4-interactions for which $f_{ij} = 0.5$, as discussed below. The parameters were adopted as much as possible from the OPLS-UA force field. Initial charges for CH_n groups were obtained from the UA charge and assignment of charges of +0.06 e to the hydrogens as for alkanes.[17] Testing for the properties of pure liquids showed that this scheme was often inadequate and some adjustments to the charges and, more rarely, to the Lennard-Jones parameters were required. Thus, the charges for the OPLS force fields are empirical and have been obtained largely from fitting to reproduce properties of organic liquids. The charges for functional groups are taken to be transferable between molecules and the use of neutral subunits makes the derivation of charges for large molecules straightforward. This represents a major difference with the AMBER94 force field[3c] for which charges are obtained on a case-by-case basis from fitting to electrostatic potential surfaces from ab initio 6-31G* calculations.

Nonbonded interactions are also evaluated for intramolecular atom pairs separated by three or more bonds. As in prior work, it was found to be necessary to scale the 1,4-nonbonded interactions to permit use of the same parameters for inter- and intramolecular interactions. Scaling factors $f_{ij} = {}^1/_2$ for both the Coulombic and Lennard-Jones interactions emerged as the final choice, which is the same as in some AMBER force fields.[3a,b] The OPLS/AMBER force field uses scaling factors of ${}^1/_2$ and ${}^1/_8$, respectively.[15] Some advantages of ${}^1/_8$ and ${}^1/_8$ were initially found here, but turned out to be problematic for molecules that can form internal hydrogen bonds including dipeptides. All nonbonded parameters for the OPLS-AA force field are reported in the Supporting Information, Tables 1−5. The previous AA nonbonded parameters reported for water and nucleoside bases can be used in conjunction with the new parameters.[10,14]

The energetics for bond stretching and angle bending are represented by eqs 2 and 3.

$$E_{\text{bond}} = \sum_{\text{bonds}} K_r (r - r_{\text{eq}})^2 \qquad (2)$$

$$E_{\text{angle}} = \sum_{\text{angles}} K_\theta (\theta - \theta_{\text{eq}})^2 \qquad (3)$$

Almost all constants in this case were taken from the AMBER all-atom force field.[3b] The principal exceptions were the parameters for alkanes that are summarized in the Supporting Information, Table 6. The listed values from a recent CHARMM force field[4] were adopted because they led to significant improvements for both structures and energetics. The values of 109.5° for the θ_{eq} of C−C−C, C−C−H, and H−C−H in the AMBER force fields were most problematic.[3b,c] Energy minimizations for ethane, propane, and butane with these parameters led to widening of the bond angles in the same order as obtained from the ab initio calculations (C−C−C > C−C−H > H−C−H). However, comparatively higher angle bending energies were obtained, which required some compensation in the torsional parameters.

(17) Kaminski, G.; Duffy, E. M.; Matsui, T.; Jorgensen, W. L. *J. Phys. Chem.* **1994**, *98*, 13077.

(18) Maxwell, D. S.; Tirado-Rives, J.; Jorgensen, W. L. *J. Comput. Chem.* **1995**, *16*, 984.

Table 1. Relative Energies (kcal/mol) for Conformations of Hydrocarbons and Alcohols

molecule	dihedral	conf	OPLS-AA	6-31G*
ethane	H−C−C−H	0	3.01	2.99
		60	0.00	0.00
propane	H−C−C−C	0	3.32	3.34
		60	0.00	0.00
butane	C−C−C−C	0	6.04	6.19
		60	1.18	1.01
		120	3.68	3.65
		180	0.00	0.00
2-methylbutane	C−C−C−C	60	0.70	0.82
		120	5.14	5.48
		180	0.00	0.00
		240	2.62	2.74
2,3-dimethylbutane	C−C−C−C	0	6.99	7.78
		60	0.01	0.00
		120	3.77	3.77
		180	0.00	0.00
cyclohexane		chair	0.00	0.00
		tb	8.53	6.76
propene	H−C−C═C	0	0.00	0.00
		180	1.93	2.07
ethylbenzene	C−C−C(ar)−C(ar)	0	1.42	1.43
		90	0.00	0.00
ethylbenzene	H−C−C−C(ar)	0	3.63	3.63
		60	0.00	0.00
methanol	H−C−O−H	0	1.36	1.36
		60	0.00	0.00
ethanol	C−C−O−H	0	1.76	1.80
		60	0.09	0.12
		120	1.32	1.32
		180	0.00	0.00
ethanol	H−C−C−O	0	3.67	3.64
		60	0.00	0.00
propanol	C−C−C−O	0	5.52	5.40
		60	0.02	0.00
		120	3.90	3.93
		180	0.00	0.08
phenol	C−C−O−H	0	0.00	0.00
		90	2.71	2.64

It was found that the resultant torsional parameters did not yield acceptable conformational energetics for 2-methylbutane and 2,3-dimethylbutane. Adoption of the angle bending constants for alkanes from CHARMM/22 led to one set of torsional parameters (Supporting Information, Table 7) that worked well for the five alkanes (Table 1).

The last intramolecular term is for the torsional energy (eq 4), where φ_i is the dihedral angle, V_1, V_2, and V_3 are the coefficients in the Fourier

$$E_{\text{torsion}} = \sum_i \frac{V_1^i}{2}[1 + \cos(\phi_i + f_i1)] + \frac{V_2^i}{2}[1 - \cos(2\phi_i + f_i2)] + \frac{V_3^i}{2}[1 + \cos(3\phi_i + f_i3)] \quad (4)$$

series, and $f1$, $f2$, and $f3$ are phase angles, which are all zero for the present systems. The total torsional energy, E_{torsion}, is then the sum of this series for each dihedral angle. The parameters that were optimized here are reported in the Supporting Information, Tables 7−9. Details on the fitting procedure are provided below.

Fitting Procedures. In order to derive the torsional parameters, the potential energy change for rotating about a bond, $E(\varphi)$, was broken into the components shown in eq 5. $E_{\text{torsion}}(\varphi)$ is the pure torsional

$$E(\phi) = E_{\text{bond}}(\phi) + E_{\text{angle}}(\phi) + E_{\text{n.b.}}(\phi) + E_{\text{torsion}}(\phi) \quad (5)$$

energy component, which consists of contributions from eq 4 for each dihedral angle involving the given bond, and the other terms represent the bond stretching, angle bending, and nonbonded interactions. The torsional parameters developed for $E_{\text{torsion}}(\varphi)$ were expected to be quite transferable between different molecular environments, since differences between related $E(\varphi)$ profiles generally stem from changes in connectivity that most affect the nonbonded energy.

For each set of torsional parameters such as the H−C−C−H, H−C−C−C, and C−C−C−C for hydrocarbons, the structures obtained at the RHF/6-31G* level[18] were analyzed at each dihedral angle to determine the energetic components of $E(\varphi)$ from the force field with the exception of $E_{\text{torsion}}(\varphi)$. This information along with a list of all dihedral values and relative energies for the ab initio structures were used as input to the program fitpar.[19] A combination of Fletcher−Powell and simplex routines[20] was applied in order to minimize the differences in relative energies calculated from the OPLS-AA force field and those obtained at the RHF/6-31G* level. The Fourier coefficients were optimized with the fitpar program for each dihedral type, unnecessary (near zero) Fourier terms were removed, and the parameters were refit. The process was repeated until the smallest number of terms was found that reasonably replicated the gas-phase energy profiles. For example, only five non-zero Fourier terms are used for all alkanes (Supporting Information, Table 7). This procedure provided a good trial set of torsional parameters which were used in the generation of structures with the BOSS program,[21] *via* its Fletcher−Powell minimization routine. The torsional parameters were then refit with the geometrical data obtained from the force-field minimized structures and ab initio energies. This multistep procedure makes the torsional energetics from the OPLS-AA force field closely match RHF/6-31G* results, as documented below. Some iteration with the liquid simulations also occurred. That is, if a set of partial charges had to be modified owing to unsatisfactory reproduction of liquid properties, the associated torsional terms had to be refit owing to changes in the other terms in eq 5, especially the nonbonded energy. If additional parameters are developed by others, it is recommended to use the same procedures, particularly 6-31G* energetics, as a basis for torsional parameters and validation of nonbonded parameters through computations of pure liquid properties and/or free energies of hydration.

Gas-Phase Calculations. The AA force field was tested in the replication of molecular structures and torsional energy profiles from ab initio calculations at the RHF/6-31G* level.[18] Key relative energies for various conformations of more than 50 ions and molecules are listed in Tables 1−6. The force-field results were obtained with BOSS for the specified value of a dihedral angle by minimizing the total energy with respect to the remaining internal degrees of freedom with a convergence criteria of 0.0001 kcal mol^{-1}. BOSS includes a dihedral driver procedure that automatically generates an optimized torsional energy profile for the designated dihedral angle. For cases in which more than one dihedral angle is needed to specify the structure, the remaining dihedral angles were assigned initial values from the global minimum. For example, for propanol in Table 1, relative energies are given for variation of the C−C−C−O angle with the C−C−O−H angle near 180°. The global minimum in each case has been previously illustrated.[18] All bond lengths, bond angles, and dihedral angles were optimized with the one constraint that trigonal carbons, amide nitrogens, and nitrogens in aromatic rings were not allowed to pyramidalize. This is easily done in BOSS by not specifying the associated dihedral angles as variable in the **Z**-matrix. It can also be done by introducing improper dihedral angles with large V_2 constants or a stiff harmonic term for out-of-plane bending.[3,7]

Liquid Simulations. The force field was also developed and validated by computing the structures and thermodynamic properties of more than 30 pure organic liquids. The Monte Carlo simulations were run with the BOSS program, version 3.6,[21] on Silicon Graphics workstations and a 200 MHz Pentium-Pro personal computer.[22] The program allows simulation of any user-specified ("custom") liquid with sampling of any or all internal degrees of freedom. In each case, a periodic box was generated containing 267 molecules. The user provides a **Z**-matrix (internal coordinate representation) of one molecule

(19) Maxwell, D.; Tirado-Rives, J. *Fitpar Version 1.1.1*; Yale University: New Haven, CT, 1994.

(20) Schlegel, H. B. *Ab Initio Methods in Quantum Chemistry*, Lawley, K. P., Ed.; Wiley: New York, 1987; pp 249−286. Nelder, J. A.; Mead, R. *Computer J.* **1965**, *7*, 308.

(21) Jorgensen, W. L. *BOSS Version 3.6*; Yale University: New Haven, CT 1995.

(22) Tirado-Rives, J.; Jorgensen, W. L. *J. Comput. Chem.* **1996**, *17*, 1385.

Table 2. Relative Energies (kcal/mol) for Conformations of Sulfur-Containing Molecules

molecule	dihedral	conf	OPLS-AA	6-31G*
methanethiol	H−C−S−H	0	1.37	1.40
		60	0.00	0.00
ethanethiol	C−C−S−H	0	1.79	1.78
		60	0.00	0.00
		120	1.56	1.54
		180	0.34	0.31
ethanethiol	H−C−C−S	0	3.65	3.62
		60	0.00	0.00
propanethiol	C−C−C−S	0	6.18	6.39
		60	1.14	0.93
		120	3.76	3.62
		180	0.00	0.00
CH_3SCH_3	H−C−S−C	0	2.13	2.13
		60	0.00	0.00
$CH_3CH_2CH_2SCH_3$	C−C−C−S	0	6.36	6.29
		60	1.00	0.94
		120	3.61	3.47
		180	0.00	0.00
$CH_3CH_2CH_2SCH_3$	C−C−S−C	0	4.43	4.49
		60	0.57	0.55
		120	1.87	1.83
		180	0.00	0.00
CH_3SSCH_3	C−S−S−C	0	10.41	11.03
		90	0.00	0.00
		180	6.00	5.37
CH_3SSCH_3	H−C−S−S	0	1.74	1.75
		60	0.00	0.00
$CH_3CH_2SSCH_3$	C−C−S−S	0	4.28	3.91
		60	0.45	0.17
		120	1.89	1.60
		180	0.00	0.00
		240	1.65	1.76
		300	0.66	0.58

Table 3. Relative Energies (kcal/mol) for Conformations of Aldehydes and Ketones

molecule	dihedral	conf	OPLS-AA	6-31G*
ethanal	H−C−C−O	0	0.00	0.00
		60	1.04	1.03
propanal	C−C−C−O	0	0.00	0.00
		60	2.01	2.05
		120	1.00	1.16
		180	1.74	1.79
propanone	H−C−C−O	0, 0	0.00	0.00
		0, 180	0.85	0.86
butanal	C−C−C−C	0	7.61	7.82
		30	5.11	4.85
		60	0.94	0.85
		90	0.97	1.26
		120	3.10	2.92
		150	1.57	1.47
		180	0.00	0.00
butanone	C−C−C−O	0	0.00	0.00
		80	1.55	1.55
		100	1.67	1.67
		180	2.91	2.91
2-aminobutanal	N−C−C−C	0	5.29	5.20
		60	0.00	0.00
		120	6.51	6.53
		180	1.97	1.40
		240	4.16	3.94
		300	0.24	0.06
2-amino-3-hydroxy-propanal	N−C−C−O	0	9.15	9.14
		60	2.33	2.53
		120	5.82	6.19
		180	0.00	0.00
		240	5.11	4.73
		300	1.12	0.99
2-amino-3-thio-propanal	N−C−C−S	0	5.07	4.76
		60	0.00	0.19
		120	7.21	7.10
		180	1.06	0.83
		240	3.50	3.32
		285	0.77	0.00
		300	0.27	0.14

of the liquid, which is replicated. The initial solvent box is created from a box of liquid argon scaled to the estimated volume of the custom solvent, with a central atom of the custom solvent molecules coincident with the argon atoms. The box size varied from approximately 26 × 26 × 26 Å for methanol to 37 × 37 × 37 Å for cyclohexane. In most cases, the intermolecular nonbonded interactions were truncated at 11 Å based on roughly the center-of-mass separations with quadratic smoothing of the interaction energy to zero over the last 0.5 Å. The cutoff for alkenes and acetals was 13 Å, while for propanol, cyclohexane, 2-methyl-2-propanol, phenol, ethyl methyl sulfide, NMA, DMA, and NMP it was extended to 15 Å. A standard correction was made for the Lennard-Jones interactions neglected beyond the cutoff.[11] All MC calculations were carried out in the NPT (isothermal, isobaric) ensemble at a pressure of 1 atm. Volume changes were attempted every 390 configurations. Calculations for ethane, propane, butane, propene, methanethiol, DME, and EME were run at their boiling points. The simulations were run for acetamide at 100 °C and at its boiling point, for NMA at 100 °C, for phenol at 25 °C (supercooled liquid) and at its boiling point, and for all other liquids at 25 °C.

Each liquid simulation consisted of at least 2×10^6 configurations of equilibration followed by 4×10^6 configurations of averaging with Metropolis sampling.[2] An additional 4×10^6 configurations of averaging were performed for methanol, propanol, 2-propanol, 2-methyl-2-propanol, ethyl methyl sulfide, propanethiol, NMA, NMP, DMA, DMM, DME, EME, THF, DEE, and cyclohexane. The radial distribution functions and key thermodynamic properties, heat of vaporization and density, of the liquids are well converged with MC simulations of this length. The reported uncertainties ($\pm 1\sigma$) were computed during the averaging stage from the fluctuations in separate averages over batches of 2×10^5 configurations.[2] The individual molecules were fully flexible, allowing for bond stretching, angle bending, and dihedral angle changes with the exception again that the geometry about trigonal carbons and amide and aromatic nitrogens was constrained to be planar. In order to compute the heats of vaporization, it was also necessary to perform MC simulations for a single molecule in the gas phase. The resultant total potential energy, $E_{intra}(g)$, was obtained to high precision from 1×10^5 configurations of equilibration, followed by 2×10^6 configurations of averaging. The ranges for intramolecular and intermolecular movements were adjusted to give acceptance ratios of 25−40% for new configurations. Overall, the force field development and testing have been a large undertaking spanning several years.

Results and Discussion

Gas-Phase Torsional Energies. The torsional energy results in Tables 1−6 from the OPLS-AA force field and from the ab initio 6-31G* calculations show excellent agreement. For all of the systems studied, the average difference between the two data sets is less than 0.2 kcal/mol. The largest individual discrepancy is for the high-energy twist boat form of cyclohexane in Table 1. Otherwise, deviations of more than 0.3 kcal/mol are rare for low-energy (0−4 kcal/mol) conformers. The precision of the fit is sufficiently high that subtleties in the 6-31G* results are well-reproduced. Some examples include the following: (1) the *trans* form of ethanol is lowest in energy, while it is the *gauche* form for ethanethiol (Tables 1 and 2), (2) the *gauche* form of butane is 1 kcal/mol above *trans*, the difference is 0.5 kcal/mol for propylamine, and *gauche* and *trans* propanol are isoenergetic (Tables 1 and 4), (3) the barriers for methyl torsions increase along the series ethanoate ion < acetamide < ethanal < methanol, methanethiol < propene < methylamine < ethane (Tables 1−6), and (4) ethylbenzene prefers a perpendicular structure, while *gauche* and *trans* minima are found for 5-ethylimidazole, and a planar structure is preferred for 3-ethylindole (Tables 1 and 4).

Application of the torsional parameters is mostly straightforward. The total number of dihedrals around each rotatable

Table 4. Relative Energies (kcal/mol) for Conformations of Amines and Ammonium Ions

molecule	dihedral	conf	OPLS-AA	**6**-31G*
methylamine	H−C−N−H	0	2.42	2.39
		60	0.00	0.00
ethylamine	C−C−N−H	60	0.02	0.06
		120	2.70	2.80
		180	0.00	0.00
		240	2.01	2.19
ethylamine	H−C−C−N	0	3.75	3.69
		60	0.00	0.00
propylamine	C−C−C−N	0	5.82	5.68
		60	0.57	0.55
		120	4.29	4.09
		180	0.00	0.00
methylammonium ion	H−C−N−H	0	2.39	2.37
		60	0.00	0.00
ethylammonium ion	C−C−N−H	0	2.64	2.63
		60	0.00	0.00
ethylammonium ion	H−C−C−N	0	3.41	3.45
		60	0.00	0.00
propylammonium ion	C−C−C−N	0	5.41	5.41
		60	0.49	0.49
		120	3.80	3.80
		180	0.00	0.00
5-methylimidazole	H−C−C−N	0	1.28	1.29
		60	0.00	0.00
5-ethylimidazole	C−C−C−N	0	1.88	1.93
		60	0.00	0.00
		120	1.04	1.11
		180	0.05	0.14
3-methylindole	H−C−C3−C2	0	0.00	0.00
		60	1.62	1.59
3-ethylindole	C−C−C3−C2	0	0.00	0.00
		60	0.76	1.17
		120	0.41	0.21
		180	3.66	4.27

Table 5. Relative Energies (kcal/mol) for Conformations of Carboxylate and Guanidinium Ions[a]

molecule	dihedral	conf	OPLS-AA	ab initio
ethanoate ion	H−C−C−O	0	0.05	0.01
		30	0.00	0.00
propanoate ion	C−C−C−O	0	0.00	0.00
		90	0.62	0.72
propanoate ion	H−C−C−C(O)	0	2.50	2.59
		60	0.00	0.00
butanoate ion	C−C−C−C	0	5.27	5.80
		60	0.08	0.07
		120	2.44	2.70
		180	0.00	0.00
guanidinium ion	H−N−C−N	0	0.00	0.00
		90	9.51	10.33
methylguanidinium ion	C−N−C−N	0	0.00	0.00
		90	10.92	12.24
methylguanidinium ion	H−C−N−C	0	1.33	1.65
		60	0.00	0.00
ethylguanidinium ion	C−C−N−C	0	7.09	6.69
		90	0.73	0.94
		120	0.78	1.64
		180	0.00	0.00

[a] Ab initio results are at the RHF/6-31+G* level for the carboxylate ions and at the RHF/6-31G* level for the guanidinium ions.

bond is given by the product of the number of attached groups on one end of the bond and the number of attached groups on the other end. In butane, for example, there are 27 dihedrals: 1 C−C−C−C, 10 H−C−C−C, and 16 H−C−C−H. Analogously, there are 30 dihedrals in 2-methyl-2-propanol: 9 H−C−C−O, 18 H−C−C−C, and 3 H−O−C−C. A special case is 5-alkylimidazoles. The parametrization was performed for 5-methylimidazole such that the H−C−C5−N1 dihedral has non-zero Fourier coefficients and the Fourier coefficients for the H−C−C5−C4 dihedral were taken as zero (Supporting Information, Table 9). Also, the torsional term for H−C−C−C(ar) in ethylbenzene (Supporting Information, Table 7) is used for the H−C−C−C5 dihedral in 5-ethylimidazole. For other aromatic systems, e.g., phenol, alkylbenzenes, and 3-alkylindoles, all dihedral terms are included about the bonds attached to the aromatic rings.

Table 6. Relative Energies (kcal/mol) for Conformations of Amides and Other Molecules

molecule	dihedral	conf	OPLS-AA	6-31G*
N-methylformamide	C−N−C−H	0	0.13	0.06
		45	0.01	0.00
		60	0.00	0.02
N-ethylformamide	C−N−C−C	0	4.73	4.75
		90	0.00	0.00
		180	0.41	0.42
N-ethylformamide	N−C−C−H	0	3.73	3.74
		60	0.00	0.00
N-propylformamide	N−C−C−C[a]	0	5.41	5.21
		60	0.31	0.29
		120	4.34	4.15
		180	0.00	0.00
acetamide	H−C−C−N	0	0.17	0.10
		45	0.03	0.00
		60	0.00	0.01
propanamide	C−C−C−N	0	1.99	1.69
		180	0.00	0.00
butanamide	C−C−C−C(O)	0	5.48	5.80
		60	0.38	0.27
		120	2.87	2.92
		180	0.00	0.00
N-methylacetamide	O−C−N−C	0	0.00	0.00
		180	2.80	2.42
ethyl methyl ether	C−O−C−C	0	6.85	6.84
		60	0.00	0.00
		180	1.37	1.67
dimethoxymethane	C−O−C−O	60, 60	0.00	0.00
		60, 120	2.73	3.32
		60, 180	2.01	2.42
acetic acid[b]	O−C−O−H	0	0.00	0.00
		90	12.01	12.55
		180	4.31	5.85

[a] C−N−C−C fixed at 180°. [b] Ab initio results for acetic acid are at the MP3/6-311+G**//6-31G* level: Wiberg, K. B.; Laidig, K. E. *J. Am. Chem. Soc.* **1987**, *109*, 5935.

Where possible, parameters were transferred to related systems. This may be seen in the case of the coefficients of H−C−C−S. Originally derived in the thiol series, the coefficients also proved acceptable for sulfides and disulfides (Supporting Information, Table 7). This is not the case with C−C−C−S, though in both series there is a substantial V_1 for this dihedral. Similarly, ethers and acetals use alcohol parameters except for the H−C−O−C, C−C−O−C, and C−O−C−O dihedrals in Table 8 in the Supporting Information. The anomeric effect is reflected in the C−O−C−O parameters. Thus, the conformer with both C−O−C−O angles at 60° is the lowest energy form for dimethoxymethane (Table 6).

Torsion about amide and peptide C(O)−N bonds is handled by the last four entries in Table 8 in the Supporting Information. These yield an *E*/*Z* energy difference for NMA of 2.8 kcal/mol (Table 6), which matches experimental data, as summarized elsewhere.[13] In general, many torsional parameters are taken to be the same for amides and peptides (Supporting Information, Tables 8 and 9). However, additional fitting for the alanine dipeptide analogue, *N*-acetyl-*N*′-methylalaninamide (acetyl-Ala-$NHCH_3$), was carried out focusing on rotation about the N−C_α and C_α−C(O) bonds. This resulted in the parameters for the φ and ψ angles in Table 9 in the Supporting Information. With OPLS-AA, the four well-defined minima in the Ramachandran map corresponding to the $C7_{eq}$, C5, $C7_{ax}$, and α' conformers

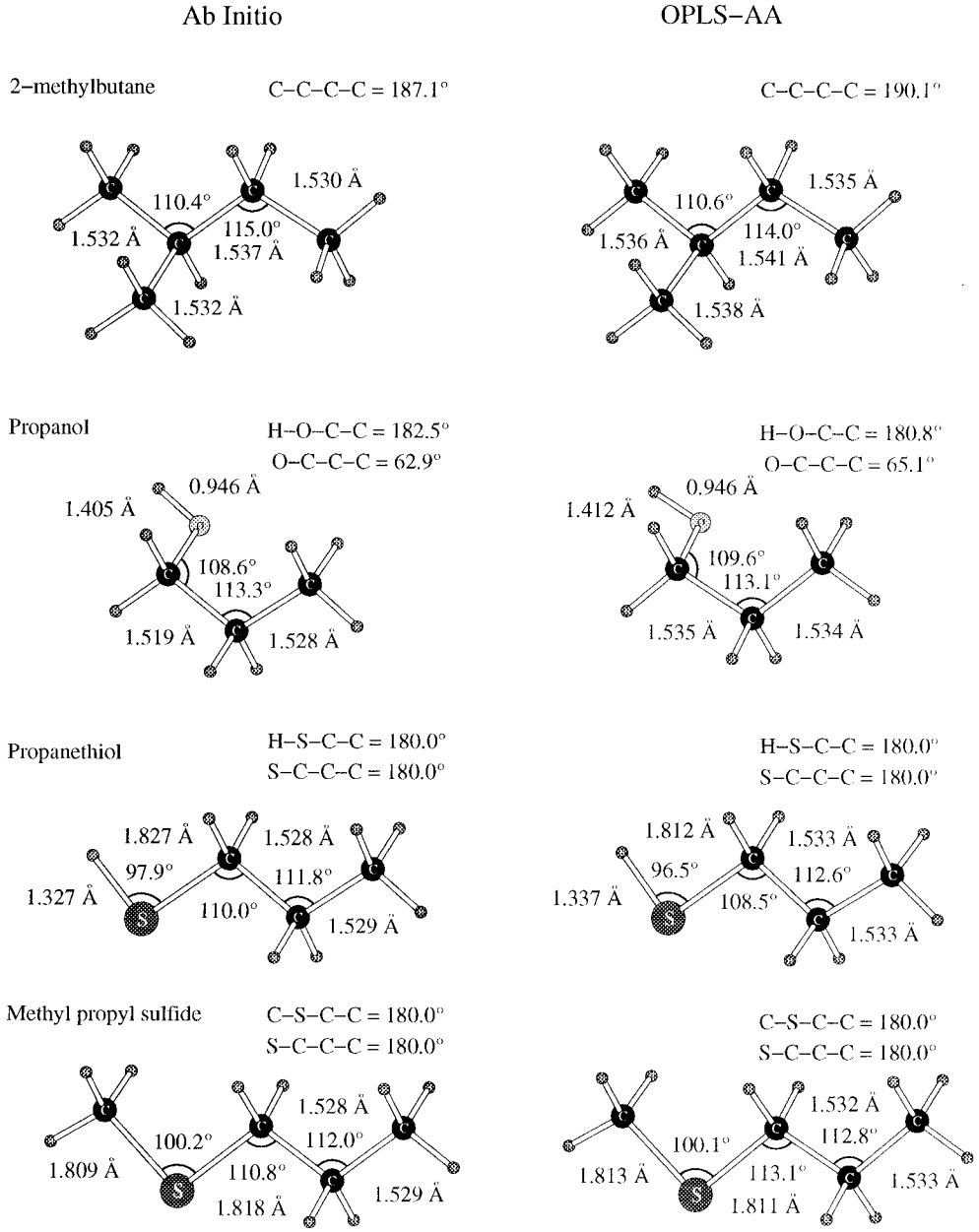

Figure 1. Optimized structures for 2-methylbutane, propanol, propanethiol, and methyl propyl sulfide from RHF/6-31G* calculations (left) and the OPLS-AA force field (right).

have relative energies of 0.00, 1.49, 2.48, and 6.74 kcal/mol. These values show little deviation from the best available ab initio results (LMP2/cc-pVTZ(-f)//MP2/6-31G*) of 0.00, 1.14, 2.68, and 5.45 kcal/mol, respectively.[23a] In fact, the differences between the OPLS-AA and these LMP2 results are about the same or less than the differences between the LMP2 results and other high-level ab initio findings, e.g., MP2/TZP//MP2/6-31G**.[23] Accord between OPLS-AA and MP2/TZP relative energies for α_R and β structures is also reasonable, while substantial discrepancies between MP2/TZP and CHARMM results have been noted.[23b]

The parameters for χ_1 of peptides in Table 9 in the Supporting Information were developed from the conformational results for the 2-aminoaldehydes in Table 3. In order to mimic polypeptides better, the backbone atoms (HCOCNH2) were constrained to be planar in this case. Though torsional parameters for the remaining peptide side chains can be taken from the present results on organic molecules, additional ab initio calculations and force-field testing for other dipeptide analogs that incorporate the remaining side chains of peptide residues are underway. As presented in detail by Friesner and co-workers,[23a] the OPLS-AA force field has been tested against the relative energetics from high-level ab initio calculations for ten conformers of an alanine tetrapeptide. The OPLS-AA, MM3*, and MMFF[7] force fields were found to perform the best among many alternatives. The lack of testing of the latter force fields for properties of organic liquids or other condensed-phase systems should be noted. In fact, results with MMFF for pure organic liquids show large errors in computed properties.[24]

Gas-Phase Structures. Structural comparisons are provided in Figures 1 and 2 for eight diverse molecules and ions. Results of full optimizations with ab initio RHF/6-31G* calculations and from BOSS with the OPLS-AA force field are shown. Computed values for key bond lengths, bond angles, and dihedral angles are given; bond lengths and angles within CH_n

(23) (a) Beachy, M. D.; Chasman, D.; Murphy, R. B.; Halgren, T. A.; Friesner, R. A. *J. Am. Chem. Soc.* In press. (b) Gould, I. R.; Cornell, W. D.; Hillier, I. H. *J. Am. Chem. Soc.* **1994**, *116*, 9250.

(24) Kaminski, G.; Jorgensen, W. L. *J. Phys. Chem.* In press.

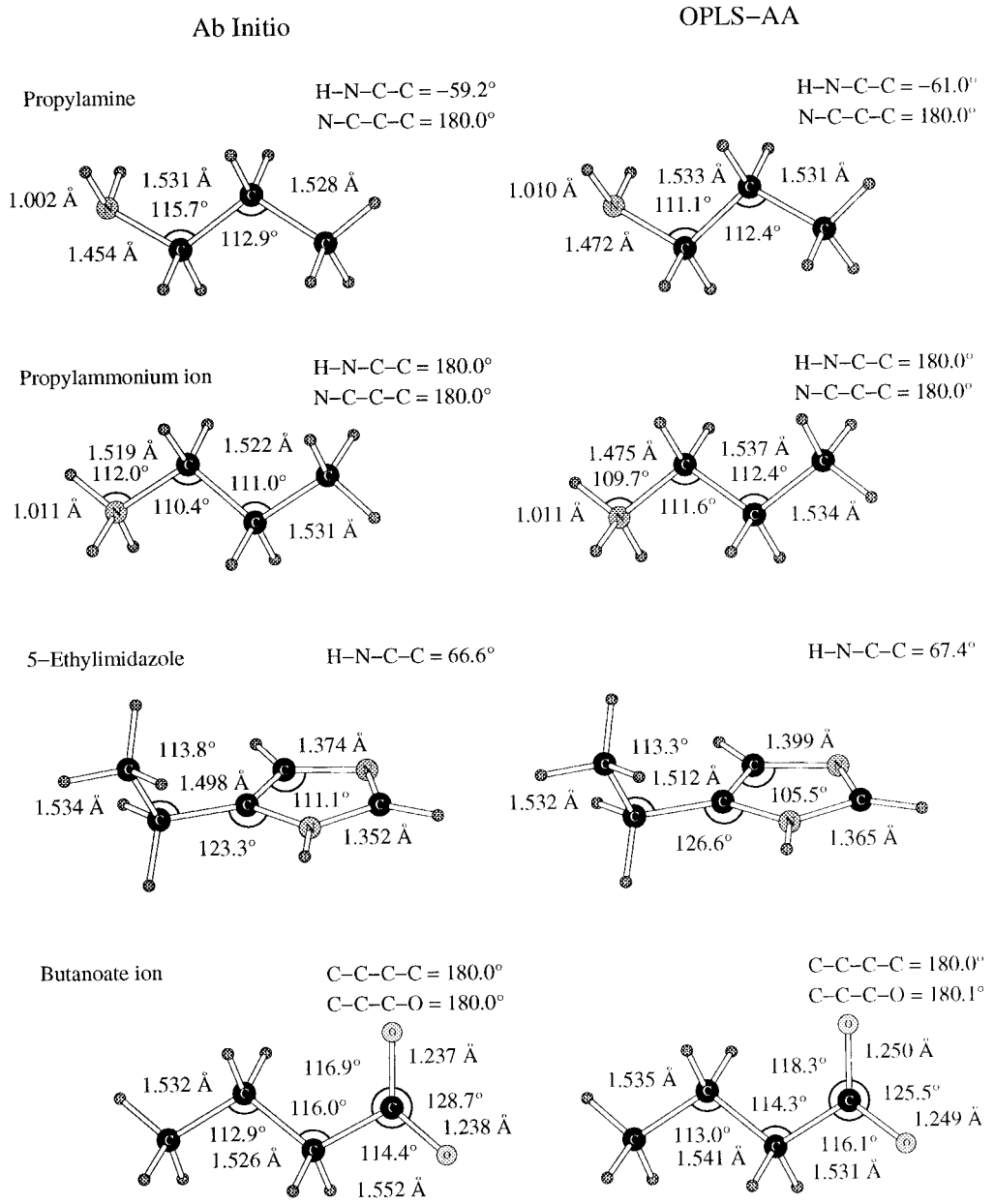

Figure 2. Optimized structures for propylamine, propylammonium ion, 5-ethylimidazole, and butanoate ion from RHF/6-31G* calculations (left) and the OPLS-AA force field (right).

groups are not shown since the differences are negligible. The molecules and ions were chosen at random except to provide representative coverage of the functional groups considered here. The predicted structures from the ab initio and force field calculations are in very close accord. It is hard to find a notable difference between the two sets of computed structures. The average differences between the RHF/6-31G* and OPLS-AA results are 0.01 Å for bond lengths, 2° for bond angles, and 1° for dihedral angles. In turn, the average differences between 6-31G* and gas-phase experimental bond lengths and bond angles are ca. 0.02 Å and 1°.[25] As illustrated, many of the C−C−C angles are near 112°, which is consistent with the CHARMM/22 value of 112.7° for θ_{eq} of CT−CT−CT that has been adopted here. In the study by Friesner and co-workers, the OPLS-AA force field was found to yield by far the best predicted structures for the tetrapeptide conformers in comparison to ab initio RHF/6-31G** results.[23a]

Liquid Properties. Key results from the simulations of each liquid are listed in Tables 7−12, along with comparisons to experimental values. The heat of vaporization, ΔH_{vap}, is calculated using eq 6, which is simply $H_{gas} - H_{liquid}$.[11]

$$\Delta H_{vap} = E_{intra}(g) - (E_{intra}(l) + E_{inter}(l)) + RT \qquad (6)$$

Assuming ideality, the pV term for the gas in $H = E + PV$ is RT, and the pV term for the liquid is negligible. $E_{intra}(g)$ was obtained from the gas-phase Monte Carlo simulations and $E_{intra}(l)$ is the average internal energy determined in the liquid simulations. $E_{inter}(l)$, the intermolecular energy in the liquid, plus $E_{intra}(l)$ equals the total potential energy of the liquid, E_{tot}.

The intermolecular component of the liquid's heat capacity at constant pressure, $C_{p(inter)}$, is calculated from fluctuations in the total intermolecular energy. Adding the ideal gas $C_p°$ obtained from experiment or ab initio calculations less R to remove the gas-phase PV contribution to $C_p°$ gives $C_p(l)$, which may be compared to the literature value. The isothermal compressibility, κ, is calculated from fluctuations in the volume.[11]

The average error for ΔH_{vap} is 2.4% or ca. 0.2 kcal/mol, while the average error for the densities is 1.6% or ca. 0.02 g cm^{-3}.

(25) Hehre, W. J.; Radom, L.; Schleyer, P. v. R.; Pople, J. A. *Ab Initio Molecular Orbital Theory*; Wiley: New York, 1986.

Table 7. OPLS-AA Energetic Results for Liquid Hydrocarbons and Alcohols[a]

liquid	T	$-E_{inter}$(l)	E_{intra}(g)	E_{intra}(l)	ΔH_{vap} calcd	ΔH_{vap} exptl
ethane	-88.63	3.07 ± 0.01	5.29 ± 0.02	5.28 ± 0.01	3.44 ± 0.02	3.52[b]
propane	−42.07	4.05 ± 0.02	8.63 ± 0.03	8.64 ± 0.02	4.50 ± 0.04	4.49[b]
butane	−0.50	4.79 ± 0.03	11.95 ± 0.07	11.84 ± 0.02	5.44 ± 0.07	5.35[b]
isobutane	25.00	4.28 ± 0.04	12.30 ± 0.07	12.29 ± 0.02	4.87 ± 0.08	4.57[b]
cyclohexane	25.00	7.34 ± 0.04	26.22 ± 0.08	26.35 ± 0.02	7.80 ± 0.09	7.86[c]
propene	−47.65	3.99 ± 0.02	5.47 ± 0.03	5.48 ± 0.01	4.43 ± 0.04	4.40[d]
trans-2-butene	25.00	4.61 ± 0.04	7.87 ± 0.03	7.85 ± 0.02	5.22 ± 0.06	5.15[b]
methanol	25.00	8.51 ± 0.02	7.08 ± 0.02	7.23 ± 0.01	8.95 ± 0.02	8.95[c]
ethanol	25.00	9.92 ± 0.04	7.13 ± 0.03	7.35 ± 0.02	10.29 ± 0.06	10.11[c]
propanol	25.00	10.74 ± 0.03	9.39 ± 0.04	9.91 ± 0.02	10.81 ± 0.05	11.31[c]
2-propanol	25.00	10.73 ± 0.03	3.97 ± 0.04	4.18 ± 0.02	11.11 ± 0.05	10.88[c]
t-BuOH	25.00	11.01 ± 0.04	−0.57 ± 0.05	-0.53±0.02	11.56±0.07	11.14[e]
phenol	25.00	13.60±0.04	8.09±0.04	8.20 ± 0.02	14.09 ± 0.06	13.82[c]
phenol	181.84	10.20 ± 0.06	11.83 ± 0.05	11.94 ± 0.03	11.00 ± 0.09	10.92[c]

[a] Temperature in °C; energies in kcal mol^{-1}. [b] Reference 29. [c] Reference 30. [d] Reference 31. [e] Reference 32.

Table 8. OPLS-AA Energetic Results for Other Liquids[a]

liquid	T	$-E_{inter}$(l)	E_{intra}(g)	E_{intra}(l)	ΔH_{vap} calcd	ΔH_{vap} exptl
CH_3SH	5.96	5.49 ± 0.02	6.15 ± 0.01	6.15 ± 0.01	6.05 ± 0.02	5.87[b]
CH_3CH_2SH	25.00	6.25 ± 0.02	6.78 ± 0.03	6.83 ± 0.00	6.79 ± 0.04	6.58[c]
$CH_3CH_2CH_2SH$	25.00	7.33 ± 0.03	10.21 ± 0.04	10.26 ± 0.02	7.88 ± 0.05	7.62[d]
CH_3SCH_3	25.00	6.46 ± 0.02	10.09 ± 0.02	10.09 ± 0.01	7.05 ± 0.03	6.61[e]
$CH_3CH_2SCH_3$	25.00	7.36 ± 0.04	9.77 ± 0.04	9.80 ± 0.02	7.93 ± 0.06	7.61[f]
CH_3SSCH_3	25.00	8.30 ± 0.03	0.12 ± 0.03	0.15 ± 0.02	8.86 ± 0.05	9.18[c]
acetamide	221.15	12.45 ± 0.05	−20.74 ± 0.05	−21.02 ± 0.03	13.71 ± 0.07	13.4[g]
acetamide	100.00	14.96 ± 0.04	−22.93 ± 0.05	−23.08 ± 0.02	15.86 ± 0.07	
NMA	100.00	12.89 ± 0.03	−6.63 ± 0.05	−6.55 ± 0.02	13.55 ± 0.06	13.3[g]
NMP	25.00	15.35 ± 0.03	−3.77 ± 0.04	−3.67 ± 0.03	15.85 ± 0.05	15.5[d]
DMA	25.00	11.46 ± 0.03	8.72 ± 0.06	8.79 ± 0.02	11.99 ± 0.07	11.75[e]
DME	−24.60	4.64 ± 0.02	8.14 ± 0.01	8.16 ± 0.01	5.15 ± 0.03	5.14[h]
EME	7.35	5.33 ± 0.03	8.01 ± 0.01	8.09 ± 0.03	5.97 ± 0.04	5.91[c]
DEE	25.00	6.09 ± 0.02	8.16 ± 0.01	8.28 ± 0.02	6.80 ± 0.05	6.56[c]
THF	25.00	6.83 ± 0.02	27.92 ± 0.01	27.98 ± 0.02	7.49 ± 0.04	7.61[e]
DMM	25.00	6.37 ± 0.03	9.31 ± 0.01	9.78 ± 0.03	7.43 ± 0.05	6.90[e]
1,3-dioxolane	25.00	8.47 ± 0.03	29.13 ± 0.01	28.81 ± 0.03	8.74 ± 0.04	8.5[e]
acetic acid	25.00	12.05 ± 0.01	−14.99 ± 0.01	−15.12 ± 0.01	12.51 ± 0.03	12.49[c]
acetic acid	100.00	10.70 ± 0.01	−13.78 ± 0.01	−13.99 ± 0.02	11.44 ± 0.03	11.30[i]
ethanal	25.00	5.67 ± 0.02	−0.37 ± 0.02	−0.32 ± 0.02	6.22 ± 0.03	6.24[e]
propanal	25.00	7.05 ± 0.03	6.19 ± 0.04	6.22 ± 0.03	7.61 ± 0.05	7.08[e]
propanone	25.00	6.71 ± 0.03	−3.22 ± 0.05	−3.16 ± 0.0.03	7.24 ± 0.06	7.48[e]
butanone	25.00	8.01 ± 0.03	2.13 ± 0.03	2.17 ± 0.02	8.56 ± 0.04	8.25[e]

[a] Temperature in °C; energies in kcal mol^{-1}. [b] Reference 33. [c] Reference 34. [d] Reference 35. [e] Reference 30. [f] Reference 36. [g] Reference 37. [h] Reference 38. [i] Reference 39.

The percentage error for C_p is noticeably higher; however, this is expected based on previous experience with fluctuation properties. A problem with the computed heat capacity arises from the approximation in separating the intermolecular and intramolecular contributions to C_p. The classical treatment of vibrations does not permit proper computation of the intramolecular contribution to C_p which necessitates the use of $C_p°$. In comparison to the united-atom model, the heat capacities from the present computations are somewhat less accurate. A likely contributor is the increased number of internal degrees of freedom in the all-atom model, which causes E_{inter} to fluctuate more.

The nonbonded parameters for the OPLS all-atom model for alkanes were previously reported.[17] The pure liquid properties were compared to those obtained using the OPLS united-atom model[11] and other all-atom models. In the present work, the box size is larger, 267 molecules instead of 128 molecules, and the bond lengths and angles were allowed to vary instead of being held rigid. Also, the prior study used a simpler form for the torsional potential with only one Fourier series for each rotatable bond instead of the separate series for each constituent dihedral angle that has been used here. Nevertheless, there are only slight differences between the present AA results and the previous ones.[17] The average errors in ΔH_{vap} for hydrocarbons

Table 9. OPLS-AA Molecular Volumes and Densities for Liquid Hydrocarbons and Alcohols[a]

liquid	T	V calc	V exptl	d calcd	d exptl
ethane	−88.63	92.8 ± 0.2	91.5	0.538 ± 0.001	0.546[b]
propane	−42.07	126.3 ± 0.4	126.0	0.580 ± 0.002	0.581[b]
butane	−0.50	164.0 ± 0.5	160.3	0.589 ± 0.002	0.602[b]
isobutane	25.00	175.1 ± 0.7	175.1	0.551 ± 0.002	0.551[b]
cyclohexane	25.00	185.1 ± 0.3	180.6	0.755 ± 0.001	0.774[c]
propene	−47.65	113.0 ± 0.2		0.618 ± 0.001	
trans-2-butene	25.00	156.9 ± 0.5	155.6	0.593 ± 0.002	0.598[b]
methanol	25.00	68.3 ± 0.1	67.7	0.779 ± 0.002	0.786[c]
ethanol	25.00	95.7 ± 0.2	97.5	0.799 ± 0.002	0.785[c]
propanol	25.00	126.2 ± 0.1	124.8	0.790 ± 0.001	0.800[c]
2-propanol	25.00	125.4 ± 0.2	127.7	0.796 ± 0.001	0.781[c]
t-BuOH	25.00	150.9 ± 0.2	157.5	0.815 ± 0.000	0.781[d]
phenol	25.00	148.8 ± 0.2	147.8	1.050 ± 0.002	1.058[e]
phenol	181.84	174.0 ± 0.5		0.898 ± 0.003	

[a] Temperature in °C; volume in Å^3 per molecule; densities in g/cm^3. [b] Reference 29. [c] Reference 30. [d] Reference 32. [e] Reference 30, based on values at 20 and 40 °C.

Table 10. OPLS-AA Molecular Volumes and Densities for Other Liquids[a]

		V		*d*	
liquid	*T*	calc	exptl	calcd	exptl
CH_3SH	5.96	89.5 ± 0.2	90.0	0.892 ± 0.002	0.888[b]
CH_3CH_2SH	25.00	120.7 ± 0.2	123.8	0.855 ± 0.002	0.833[c]
$CH_3CH_2CH_2SH$	25.00	148.2 ± 0.4	151.3	0.853 ± 0.002	0.836[d]
CH_3SCH_3	25.00	124.5 ± 0.2	122.5	0.828 ± 0.001	0.842[e]
$CH_3CH_2SCH_3$	25.00	153.1 ± 0.3	151.1	0.826 ± 0.002	0.837[c]
CH_3SSCH_3	25.00	151.7 ± 0.2	148.0	1.031 ± 0.002	1.057[c]
acetamide	221.15	109.3 ± 0.3		0.897 ± 0.003	
acetamide	100.00	96.9 ± 0.1	99.9	1.012 ± 0.001	0.981[f]
NMA	100.00	133.9 ± 0.1	135.9	0.907 ± 0.001	0.894[g]
NMP	25.00	154.1 ± 0.1	155.5	0.939 ± 0.000	0.931[h]
DMA	25.00	158.7 ± 0.1	154.5	0.911 ± 0.001	0.936[h]
DME	−24.60	106.5 ± 0.1	104.1	0.717 ± 0.002	0.735[i]
EME	7.35	140.5 ± 0.1	138.5	0.709 ± 0.003	0.721[j]
DEE	25.00	173.5 ± 0.1	173.9	0.708 ± 0.002	0.708[k]
THF	25.00	139.8 ± 0.2	136	0.855 ± 0.003	0.884[l]
DMM	25.00	147.1 ± 0.3	148	0.858 ± 0.003	0.854[h]
1,3-dioxolane	25.00	117.7 ± 0.1	116	1.045 ± 0.003	1.060[m]
acetic acid	25.00	94.1 ± 0.1	95.5	1.059 ± 0.002	1.044[n]
acetic acid	100.00	101.7 ± 0.1	104.1	0.981 ± 0.002	0.958[n]
ethanal	25.00	96.2 ± 0.2	94.8	0.761 ± 0.002	0.772[h]
propanal	25.00	122.7 ± 0.2	121.9	0.786 ± 0.002	0.791[h]
propanone	25.00	121.2 ± 0.2	123.0	0.795 ± 0.001	0.784[h]
butanone	25.00	148.8 ± 0.2	149.7	0.805 ± 0.001	0.800[h]

[a] Temperature in °C; volume in Å^3 per molecule; densities in g/cm^3. [b] Reference 40. [c] Reference 41. [d] Reference 42. [e] Reference 43. [f] Reference 30, based on values at 91−132 °C. [g] Reference 37. [h] Reference 30. [i] Reference 44. [j] Reference 45. [k] Reference 34. [l] Reference 46. [m] Reference 30, based on density at 20 °C and assumed $\alpha = 0.001$ deg^{-1}. [n] Reference 47.

Table 11. OPLS-AA Heat Capacities and Compressibilities for Liquid Hydrocarbons and Alcohols[a]

			C_p(l)		
liquid	*T*	$C_p°$	calcd	exptl	$10^6\kappa$
ethane	−88.63	8.6[b]	15.9 ± 1.0	17.6[b]	166 ± 19
propane	−42.07	14.0[b]	22.8 ± 1.2	23.5[b]	153 ± 18
butane	−0.50	21.9[b]	31.0 ± 1.3	31.8[b]	179 ± 23
isobutane	25.00	23.1[b]	38.2 ± 2.6	33.8[b]	416 ± 72
cyclohexane	25.00	25.4[c]	43.7 ± 2.3	37.3[c]	136 ± 15
propene	−47.65	10.5[d]	21.9 ± 1.9	21.9[e]	188 ± 24
trans-2-butene	25.00	21.0[b]	34.5 ± 2.2	30.5[b]	330 ± 51
methanol	25.00	10.5[c]	26.0 ± 1.8	19.5[c]	77 ± 8
ethanol	25.00	15.6[c]	35.6 ± 3.3	26.9[c]	92 ± 13
propanol	25.00	20.8[c]	35.1 ± 2.0	34.4[c]	57 ± 6
2-propanol	25.00	21.2[c]	35.9 ± 2.0	37.0[c]	59 ± 7
t-BuOH	25.00	27.1[e]	49.4 ± 3.5	52.6[f]	57 ± 7
phenol	25.00	24.7[c]	50.2 ± 4.4		65 ± 9
phenol	181.84				99 ± 28

[a] Temperature in °C; C_p in cal/(mol deg); κ in atm^{-1}. [b] Reference 29. [c] Reference 30. [d] Computed using RHF/6-31G* vibrational frequencies. [e] Reference 31. [f] Reference 32.

are 2% from both the OPLS-AA and OPLS-UA models. For densities, the errors are 3% from OPLS-AA and 2% from OPLS-UA. However, the good accord is achieved with many fewer nonbonded parameters in the AA force field. For alkanes, there are only two sets of Lennard-Jones parameters with the AA force field, one for C and one for H (Supporting Information, Table 1), while in the UA force field there are seven sets of united CH_n parameters depending on *n* and the connectivity of the adjacent carbon.[11]

The OPLS-UA model for alcohols was tested on the five saturated alcohols in Table 7 and yielded errors of only 1.3% for ΔH_{vap} and 1.8% for densities.[12a] The corresponding errors for alcohols with the AA model are 2.2% and 1.8%. An annoyance with the AA results is the incorrect ordering of the ΔH_{vap} and density for propanol and 2-propanol. The UA model

Table 12. OPLS-AA Heat Capacities and Compressibilities for Other Liquids[a]

			C_p(l)		
liquid	*T*	$C_p°$	calcd	exptl	$10^6\kappa$
CH_3SH	5.96	11.7[b]	21.7 ± 1.1	21.3[c]	175 ± 4
CH_3CH_2SH	25.00	17.4[d]	35.8 ± 2.7	28.2[d]	155 ± 19
$CH_3CH_2CH_2SH$	25.00	22.8[e]	38.3 ± 2.2		166 ± 27
CH_3SCH_3	25.00	17.4[f]	27.2 ± 1.2	28.2[f]	101 ± 12
$CH_3CH_2SCH_3$	25.00	22.7[g]	37.9 ± 2.6	34.6[g]	138 ± 22
CH_3SSCH_3	25.00	22.5[d]	34.6 ± 1.8	34.9[d]	88 ± 11
acetamide	221.15				121 ± 19
acetamide	100.00				41 ± 5
NMA	100.00	24.8[h]	39.7 ± 1.2		47 ± 4
NMP	25.00				40 ± 4
DMA	25.00	26.0[i]	41.2 ± 1.5	42.0[j]	50 ± 4
DME	−24.60	15.4[f]	25.3 ± 1.0	24.5[f]	142 ± 12
EME	7.35	21.8[d]	36.9 ± 1.7		159 ± 18
DEE	25.00	28.5[f]	39.0 ± 1.2	41.2[f]	122 ± 61
THF	25.00	18.2[f]	31.9 ± 1.5	29.6[f]	107 ± 48
DMM	25.00	22.7[k]	46.3 ± 4.2	38.6[f]	130 ± 19
1,3-dioxolane	25.00	15.2[k]	26.4 ± 1.5	28.2[l]	52 ± 5
acetic acid	25.00	15.2[f]	30.6 ± 1.4	29.4[f]	41 ± 3
acetic acid	100.00	18.0[m]	31.4 ± 1.5	33.0[n]	68 ± 7
ethanal	25.00	13.2[f]	23.5 ± 1.8	21.3[f]	124 ± 17
propanal	25.00	18.5[f]	31.0 ± 1.8	32.8[f]	110 ± 14
propanone	25.00	17.8[f]	29.5 ± 1.7	29.9[f]	120 ± 17
butanone	25.00	24.7[f]	37.4 ± 1.5	38.0[f]	86 ± 9

[a] Temperature in °C; C_p in cal/(mol deg); κ in atm^{-1}. [b] Reference 48. [c] Reference 33. [d] Reference 34. [e] Reference 49. [f] Reference 30. [g] Reference 36. [h] Reference 50. [i] Reference 30, at 27 °C. [j] Reference 30, at 20 °C. [k] Computed using RHF/6-31G* vibrational frequencies. [l] Reference 51. [m] Reference 52. [n] Reference 39.

gets the correct orderings, though the differences are smaller than from experiment. Thus, there is a problem here with branching, though the AA results for isosteric butane and isobutane show the correct orders. It may be noted that the charge separation between the oxygen and hydrogen is the same as in the UA model; however, the charge on oxygen is now less negative, −0.683 vs −0.700 e. The lessened charge and an increase in the σ for oxygen from the UA 3.07 to 3.12 Å were found to be necessary to better fit the heats of vaporization. It was still possible to use the same charges and Lennard-Jones parameters for the oxygen and hydroxyl hydrogen (Supporting Information, Table 1) for all saturated alcohols. If this simplification were abandoned, the propanol/2-propanol ordering could be fixed. Computed O−H radial distribution functions (rdfs) are shown in Figure 3. The two peaks at 1.8−1.9 and 3.4 Å reflect the nearest-neighbor hydrogen bonds; the first peak is the hydrogen bond and the second peak is for the distance between the oxygen of the hydrogen-bond donor and the hydrogen of the acceptor. The integrals of the first peak in the O−H rdfs out to the minima at 2.7 Å give half the total number of hydrogen bonds per monomer and are 0.95−1.00 in each case except for 2-methyl-2-propanol for which the value is 0.88. Of course, this reflects the presence of hydrogen-bonded chains that have been noted in crystal structures and in computer simulations of liquid alcohols.[12a] The complete set of rdfs from the OPLS-UA and AA models for alcohols show negligible differences in numbers, locations, and integrals of peaks. The only difference is that the peak heights are smaller with the AA force field, e.g., by ca. 20% for the O−H rdfs. This presumably results from the lessened charge on oxygen and perhaps the introduction of angle bending for the monomers in the AA model. The bond stretching in the present AA results has no observable effects on rdfs and only small effects on the computed thermodynamic properties, e.g., ΔH_{vap} and the density for 2,2,2-trifluoroethanol are increased by 2% and 1% for the

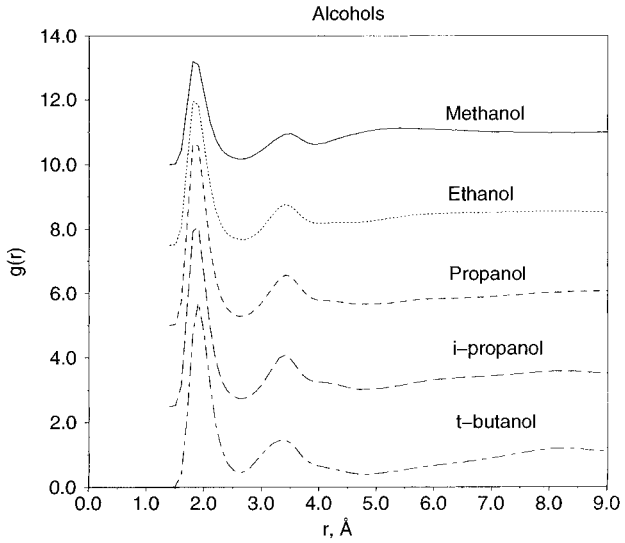

Figure 3. $O-H_O$ radial distribution functions for liquid alcohols. Successive curves are offset 2.5 units along the *y*-axis.

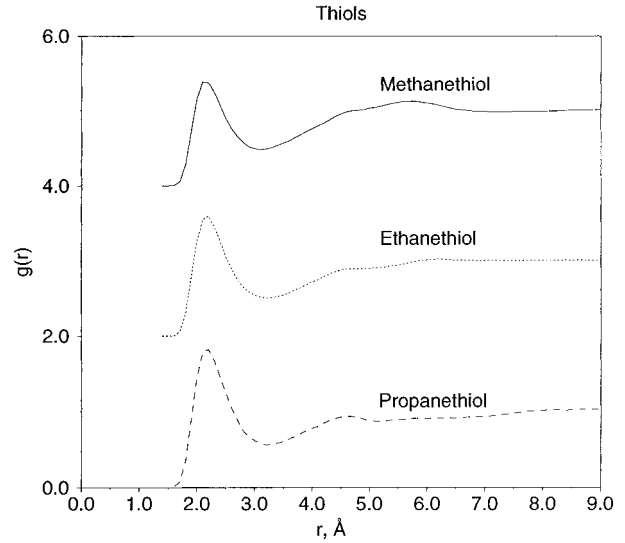

Figure 4. S−H radial distribution functions for the thiols. Successive curves are offset 2.0 units along the *y*-axis.

fully flexible AA model compared to one with bond lengths fixed at the equilibrium values.[26]

For the liquid sulfur compounds, the values for ΔH_{vap} and density are improved in going from the UA[12b] to the AA model (Tables 8 and 10). This is mainly due to progress with the properties for sulfides, especially dimethyl sulfide. The charge on sulfur is more positive by 0.015, 0.035, and 0.0825 e in the AA model for thiols, sulfides, and disulfides, respectively. However, the charge difference between sulfur and hydrogen in the thiols is the same as in the UA case. The S−H radial distribution functions for the three thiols are shown in Figure 4. The first peak near 2.2 Å integrates to 0.9 for methanethiol and ethanethiol, but to only 0.8 for propanethiol. There is little structure beyond the first peak in the S−H rdfs. The S−H rdfs for methanethiol and ethanethiol are essentially identical from the AA and UA models.[12b] The weaker, less directional hydrogen bonding for thiols than alcohols is apparent in the broader, less-sharp first peaks and vanishing second peaks in the S−H vs O−H rdfs. The S−S rdfs for the sulfides and disulfides, as presented in Figure 5, feature a broad first peak centered near 5.2 Å and are similar to the UA results.[12b] For

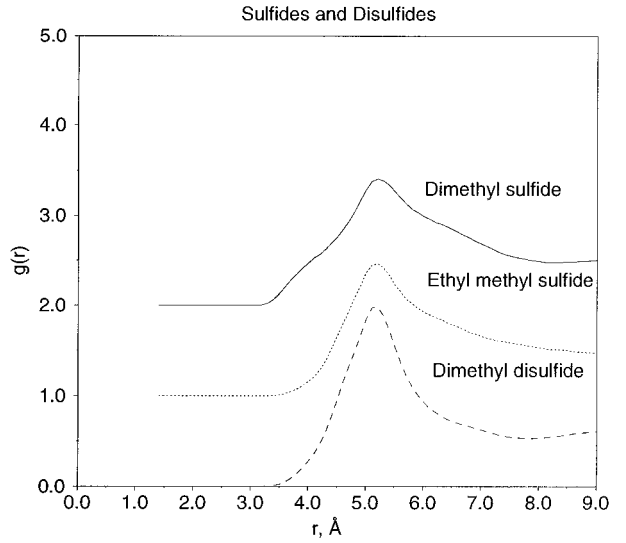

Figure 5. S−S radial distribution functions for the sulfides and disulfides. Successive curves are offset 1.0 units along the *y*-axis.

dimethyl sulfide, the main peak is preceded by a small band from 3.2 to 4.2 Å. This band is not as developed in the UA case. The density is improved with the AA model and is 7% higher than from the UA results.[12b] The leading edge in the S−S rdf likely results from greater population of bifurcated (Me_2S---Me_2S) structures at the higher density. Another noticeable difference between the rdfs for the AA and UA models occurs for dimethyl disulfide. In the UA case, the first band extends into a second one centered near 6.5 Å.[12b] The second band is not evident in the AA results. In this case, the density is 5% lower with the AA force field, which accompanied by the lessened charge on sulfur, diminishes the packing requirements in the liquid.

The AA parameters for ethers perform well in reproducing the observed densities and heats of vaporization of DME, EME, DEE, and THF with average errors of 1.8% and 1.6%, respectively (Tables 8 and 10). The OPLS-UA model does well too with corresponding errors of 1.6% and 3.0%, the principal problem occurring with DEE.[12c] For the AA model, only H−C−O−C and C−C−O−C torsional parameters needed to be introduced (Supporting Information, Table 8), while alcohol parameters are used for the additional dihedrals. A significant change is that the magnitudes of the charge, σ, and ϵ for ether O were all reduced to −0.400 e, 2.900 Å, and 0.140 kcal/mol (Supporting Information, Table 5) from the UA values of −0.500 e, 3.000 Å, and 0.170 kcal/mol. Nevertheless, the optimal interaction energy for a TIP4P water molecule with AA DME of −5.57 kcal/mol is still similar to the UA and RHF/6-31G* values of −5.77 and −5.73 kcal/mol.[12c] As discussed previously,[12c] there is little notable structure in the rdfs for liquid ethers. Lennard-Jones AA parameters for ethers were used for acetals as well. The torsional parameters for C−O−C−O for acetals (Supporting Information, Table 8) have been taken from extensive work on the OPLS-AA force field for carbohydrates, which will be described elsewhere.[27] The nonbonded parameters were validated in the MC simulations of dimethoxymethane (DMM) and 1,3-dioxolane (Tables 8, 10, and 12). Furthermore, the Lennard-Jones parameters for the COOH unit of carboxylic acids were taken without change from the UA force field;[12d] however, the magnitudes of the charges on the carbon and oxygens have been reduced by 0.03−0.06 e in the AA force field. The computed thermodynamic results for acetic acid are

(26) Duffy, E. M. Ph.D. Thesis, Yale University, 1994. Duffy, E. M. Unpublished results.

(27) Jorgensen, W. L.; Damm, W.; Frontera, A.; Tirado-Rives, J. To be submitted for publication.

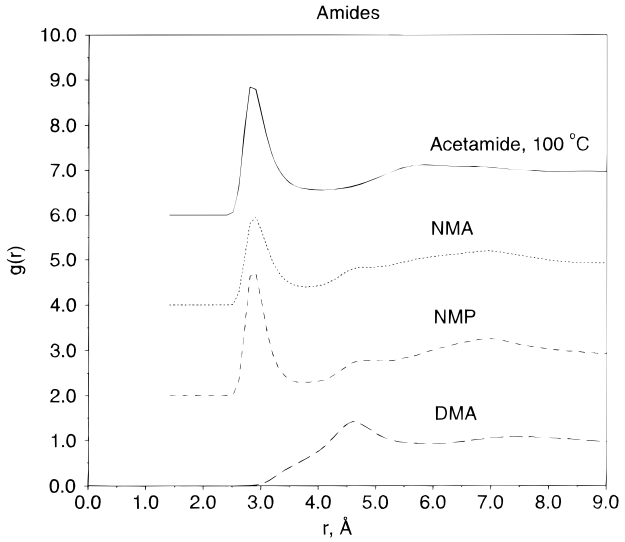

Figure 6. N−O radial distribution functions for the amides. Successive curves are offset 2.0 units along the *y*-axis.

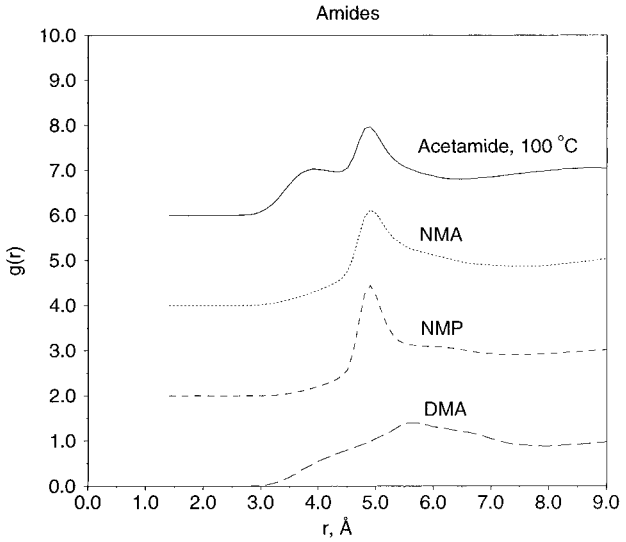

Figure 7. O−O radial distribution functions for the amides. Successive curves are offset 2.0 units along the *y*-axis.

very close to the experimental values at both 25 and 100 °C in Tables 8, 10, and 12. Description of the structure and hydrogen bonding in liquid acetic acid has been presented previously and remains unchanged.[12d]

For amides, the Lennard-Jones parameters for the CONH group and the charges for the CO unit were taken from the UA force field.[13] The magnitudes of the charges on nitrogen and the attached hydrogens are again smaller for the AA model, and the nitrogen becomes less negative in progressing from a primary to a tertiary amide (Supporting Information, Table 4). In the UA model, the charge for secondary and tertiary amide nitrogens is the same (−0.57 e), but primary amide nitrogens have a charge of (−0.85 e).[13] To reproduce the observed ΔH_{vap} of DMA, it was necessary to reduce the magnitude of the charge on nitrogen to −0.140 e in the AA force field. The normal charge of 0.06 e was kept on the alkyl hydrogens, making the charge −0.110 e on the *N*-methyl carbons. The errors for the computed heats of vaporization and densities for liquid acetamide, NMA, NMP, and DMA in Tables 8 and 10 are 2.1% and 2.0%, respectively. The only one of these liquids that was previously modeled with the UA force field was NMA, though formamide and DMF were also treated.[13] The N−O rdfs for the amides are presented in Figure 6. The first peaks at 2.9 Å for acetamide, NMA, and NMP mostly reflect the hydrogen bonding, which is absent for DMA. Integration of the first peaks to the minima yields 2.5, 1.1, and 1.0 contacts for acetamide, NMA, and NMP, respectively. Since the number of hydrogen bonds per monomer is about 2.5 for primary amides and 2.0 for secondary ones, the first peak for acetamide contains contributions from other than the hydrogen-bonded neighbors, as found previously for formamide.[13] The O−O rdfs for amides are distinctive (Figure 7). The two peaks near 4 and 5 Å for acetamide arise, as for formamide,[13] from hydrogen bonding to the hydrogens *cis* and *trans* to the oxygen, respectively. Consistently, the first peak disappears for NMA and NMP. As with the N−O rdf for liquid DMA, the O−O rdf for DMA reflects diminished structure. Further details on the structure and hydrogen bonding for liquid amides can be found in the earlier UA paper.[13]

OPLS-AA parameters are also provided for aldehydes and ketones. The results for liquid acetaldehyde, propanal, acetone, and butanone show good accord with the experimental data in Tables 8, 10, and 12. The parametrization was more trying in this case. An initial parametrization with charges of ±0.37 e for the carbonyl C and O yielded acceptable gas-phase energetics and pure liquid properties. However, the dipole moments were suspiciously close to observed gas-phase data, while OPLS values are usually enhanced by ca. 15%. This suggested that the free energies of hydration could be in error, so the difference in free energies of hydration of acetaldehyde and ethane was computed in TIP4P water using standard methods.[16] As suspected, acetaldhyde was not hydrophilic enough by 2−3 kcal/mol. The problem was remedied by enhancing the charges on carbonyl C and O to ±0.45 e for aldehydes and ±0.47 e for ketones. However, for the properties of the pure liquids to remain reasonable, attraction from another source had to be diminished. A solution was found by reducing the Lennard-Jones ϵ from 0.030 to 0.015 kcal/mol for the α and aldehyde hydrogens and by using the sp^2 C−H σ of 2.42 Å instead of the usual sp^3 C−H value of 2.50 Å (Supporting Information, Table 5). This is reminiscent of the practice with AMBER94 of reducing R* for an sp^3 H by 0.1 Å for each attached heteroatom.[3c]

Intramolecular Energetics. A final point that can be addressed from the present, large collection of results on organic liquids concerns condensed-phase effects on the internal energies. This would arise primarily from changes in conformer populations in the pure liquids vs the gas phase with higher populations of more polar forms in the condensed phase.[28] For example, this occurs for 1,2-dichloroethane for which the *gauche* population increases from 21% in the gas phase to 74% in acetonitrile.[9] Another possibility would be some intramolecular distortion to yield stronger intermolecular interactions, particularly hydrogen bonding. Recall that the molecules in the present calculations are completely flexible except for the planarity constraint on trigonal centers. The items to compare are E_{intra}(g) and E_{intra}(l) in Tables 7 and 8. For the hydrocarbons, ethers, aldehydes, ketones, and sulfur compounds, there are insignificant

(28) For a review, see: Jorgensen, W. L. *J. Phys. Chem.* **1983**, *87*, 5304.
(29) *Selected Values of Physical and Thermodynamic Properties of Hydrocarbons and Related Compounds*; American Petroleum Institute Research Project 44: Carnegie Press: Pittsburgh, 1953. *Physical Constants of Hydrocarbons*, ASTM Technical Publication No. 109A; American Society for Testing and Materials: Philadelphia, 1963.
(30) Riddick, J. A.; Bunger, W. B.; Sakano, T. K. *Techniques of Chemistry, Vol. II: Organic Solvents, Physical Properties and Methods of Purification*, 4th ed.; Wiley: New York, 1986.
(31) Powell, T. M.; Giauque, W. F. *J. Am. Chem. Soc.* **1939**, *61*, 2366.
(32) Wilhoit, R. C.; Zwolinski, B. J. *J. Phys. Chem. Ref. Data, Suppl.* **1973**, 2.

differences between the internal energies in the gas and liquid phases. This was also the usual finding with the UA force field.[11,12b,c] Changes in polarity with conformation are negligible in these cases. For much larger molecules, some self-solvation could be expected to yield relatively higher populations of more compact, low-energy conformers in the gas phase than in the liquids. Interestingly, the amides also show no significant changes in internal energies. The methyl torsions for acetamide, NMA, and DMA are nearly barrierless, so these amides essentially populate only one conformer. Furthermore, since the primary and secondary amides form 2-3 hydrogen bonds it is apparent that hydrogen bonding in these systems is not a sufficiently strong driving force to distort the molecular geometries.

For alcohols, there is more variation, though the changes in internal energy are still small. For methanol, the 0.15 kcal/mol higher internal energy in the liquid comes primarily from bond stretching (0.10 kcal/mol) and angle bending (0.04 kcal/mol). So, there is slight expansion of the hydroxyl group in the liquid to enhance the hydrogen bonding. This is consistent with the 2% increase in the ΔH_{vap} for 2,2,2-trifluoroethanol when bond stretching is allowed, which was mentioned above. Thus, all of the alcohols show somewhat higher internal energies for the liquids than in the gas phase. The effect is less for 2-methyl-2-propanol. A lower internal energy for this liquid was found in the MC simulation with the UA potential functions and comes from narrowing of the conformational wells (populating C−C−O−H angles nearer the minima at 60°, 180°, and 300°) to provide less steric hindrance to hydrogen bonding.[12a]

Conclusion

The development and testing of the OPLS all-atom force field has been described. Both nonbonded and torsional energy parameters were derived to reproduce gas-phase structures and conformational energetics from ab initio RHF/6-31G* calculations and observed thermodynamic properties of organic liquids. Multiple compounds of the same type were considered in the fitting process to avoid biasing the torsional parameters for particular molecules. The quality of the fits and the breadth and quantity of data considered are notable. The importance of testing force fields that are intended for condensed-phase simulations including protein dynamics on liquid properties has been reiterated. The OPLS-AA force field is broadly applicable, more extensively developed, and tested on conformational energetics than the OPLS-UA model, and along with the OPLS-UA model more thoroughly documented to give highly accurate descriptions of fluids than any other force fields. Little effort is required to set up a MC simulation of a pure liquid with a program like BOSS and the simulation at one temperature and pressure can be completed typically in a few hours on workstations or Pentium-based personal computers. Thus, there is no reason to not include such testing in force field development. The present paper has provided MC results for an unprecedented number of organic liquids including, for the first time, fully flexible molecules. Besides supporting the OPLS-AA model and prior views on liquid structure, this has unequivocally demonstrated that negligible solvent effects on internal energies are the rule for organic systems. Exceptions require pronounced changes in electrostatic interactions for different conformers.[9,28] There has also been independent testing on the structure and energetics for a tetrapeptide that has strikingly confirmed the quality of the OPLS-AA model.[23a] In addition, computations of free energies of hydration with the OPLS-AA and TIP4P potential functions have been completed for alkanes,[17] methanol, methanethiol, acetaldehyde, and dimethyl ether and show average errors of less than 0.5 kcal/mol. These studies will be expanded and parameters for other functionality including carbohydrates[27] will be reported.[53]

Acknowledgment. Gratitude is expressed to the National Institutes of Health and Office of Naval Research for support of this work and to Dr. A. Frontera, Dr. P. R. Rablen, and R. C. Rizzo for computational assistance.

Supporting Information Available: Tables of the nonbonded and torsional parameters for the OPLS-AA force field (12 pages). See any current masthead page for ordering and Internet access instructions.

JA9621760

(33) Russell, H., Jr.; Osborne, D. W.; Yost, D. M. *J. Am. Chem. Soc.* **1942**, *64*, 165.
(34) Wagman, D. D.; Evans, W. H.; Parker, V. B.; Schumm, R. H.; Halow, L.; Bailey, S. M.; Churney, K. L.; Nuttall, R. L. *J. Phys. Chem. Ref. Data Suppl. 2* **1982**, *11*, 1.
(35) Majer, V.; Svoboda, V. *Enthalpies of Vaporization of Organic Compounds, IUPAC Chemical Data Series No. 32*; Blackwell Scientific Publications: Oxford, 1985.
(36) Scott, D. W.; Finke, H. L.; McCullough, J. P.; Gross, M. E.; Williamson, K. D.; Waddington, G.; Huffmann, H. M. *J. Am. Chem. Soc.* **1951**, *73*, 261.
(37) Lemire, R. J.; Sears, P. G. *Top. Curr. Chem.* **1978**, *74*, 45.
(38) Kennedy, R. M.; Sagenkahn, M.; Aston, J. G. *J. Am. Chem. Soc.* **1941**, *63*, 2267.
(39) Armitage, J. W.; Gray, P. *Trans. Faraday Soc.* **1962**, *58*, 1746.
(40) Berthoud, A.; Brum, R. *J. Chim. Phys. Phys.-Chim. Biol.* **1924**, *21*, 143.
(41) Haines, W. E.; Helm, R. V.; Bailey, C. W.; Ball, J. S. *J. Phys. Chem.* **1954**, *58*, 270.
(42) Mathias, S. *J. Am. Chem. Soc.* **1950**, *72*, 1897.
(43) Haines, W. E.; Helm, R. V.; Cook, G. L.; Ball, J. S. *J. Phys. Chem.* **1956**, *60*, 549.
(44) Maass, O.; Boomer, E. H. *J. Am. Chem. Soc.* **1922**, *44*, 1709.
(45) Aronovich, K. A.; Kastorskii, L. P.; Fedorova, K. F. *Zh. Fiz. Khim.* **1967**, *41*, 20.
(46) Franks, F.; Quickenden, M. A. J.; Reid, D. S.; Watson, B. *Trans. Faraday Soc.* **1970**, *66*, 582.
(47) Hales, J. L.; Gundry, H. A.; Ellender, J. H. *J. Chem. Thermodyn.* **1983**, *15*, 211.
(48) Barrow, G. M.; Pitzer, K. S. *Ind. Eng. Chem.* **1949**, *41*, 2737.
(49) Benson, S. W.; Cruickshank, F. R.; Golden, D. M.; Haugen, G. R.; O'Neal, H. E.; Rodgers, A. S.; Shaw, R.; Walsh, R. *Chem. Rev.* **1969**, *69*, 279.
(50) Benson, S. W. *Thermochemical Kinetics*; Wiley: New York, 1976.
(51) Clegg, G. A.; Melia, T. P. *Polymers* **1969**, *10*, 912.
(52) Chao, J.; Zwolinski, B. J. *J. Phys. Chem. Ref. Data* **1976**, *7*, 363.
(53) Computer files containing all parameters for the OPLS-AA force field are available by anonymous ftp after contacting W.L.J. at bill@adrik.chem.yale.edu.